Chemical Engineering Journal 107 (2005) 45–53

Chemical Engineering Journal

www.elsevier.com/locate/cej

Total oxidation of methane over Pd catalysts supported on silicon nitride Influence of support nature

I. Kurzina[a,*], F.J. Cadete Santos Aires[b], G. Bergeret[b], J.C. Bertolini[b]

[a] *Tomsk State University of Civil Engineering, 2 Solyanaya pl., Tomsk 634003, Russia*
[b] *Institut de Recherches sur la Catalyse, 2 Av. A. Einstein, 69626 Villeurbanne Cedex, France*

Abstract

Non-oxide refractory materials such as silicon nitride showing high thermal stability and thermal conductivity can be used as catalytic supports. Silicon nitride with different specific area and crystallinity: amorphous silicon nitride (SiN-am), amorphous silicon nitride annealed at 1450 °C (120 min) under nitrogen flow (SiN-annl) and α-Si_3N_4 were chosen as supports for Pd catalysts. Commercial amorphous silicon nitride contains a small amount of crystalline phase with α/β Si_3N_4 ratio of 2.3. Annealing of the amorphous silicon nitride leads to changes in the phase composition, as well as in the morphology of the powder. An increase of the amount of crystalline phases up to 80% with α/β Si_3N_4 ratio of 6.6 was obtained after annealing. Palladium catalysts were prepared by impregnation of Pd(II) acetylacetonate in toluene solution of silicon nitride powder and were tested in the methane total oxidation reaction. A strong influence of the phase composition and the crystalline state of supports on the catalytic properties of Pd catalysts was found. The activity of Pd catalysts deposited on the amorphous Si_3N_4 is very poor. It increases with the α-Si_3N_4 content of the support.

Keywords: Pd catalyst; Silicon nitride; Oxidation reaction

1. Introduction

Highly dispersed main group metals oxides such as Al_2O_3, SiO_2 and silica–alumina are generally used as catalyst supports [1]. However, the structural stability of such catalysts for highly exothermic reactions working at high temperature (for instance the total oxidation of methane) is not sufficient. One possible reason for the instability of oxides at high temperatures might be the rather low thermal conductivity of these insulating compounds. In order to improve the stability of catalysts, other materials having high thermal stability and high thermal conductivity should be employed as supports. Among the alternative supports, silicon carbides and nitrides showed some interesting properties. Thus, transition metals supported on SiC have been investigated in carbon monoxide hydrogenation [2] and for total oxidation of methane [3]. It has been shown that oxidation of SiC occurred only at high temperature in the presence of oxygen in reaction conditions [3]. In several papers, some nitrides (oxynitrides [4], metallophosphate oxynitrides [5], zirconium oxynitrides [6]) were investigated as catalyst supports for the Knoevenagel condensation reaction. Among the non-oxide ceramics, silicon nitride is a promising candidate for high temperature applications [7] owing to its advantageous properties, like rather high thermal conductivity, high hardness and strength, excellent creep, oxidation and corrosion resistance, as well as its low density. Till now there are few relevant studies on the use of silicon nitride as a catalytic support. One can suggest that stability and activity of metal catalysts deposited on silicon nitride will depend on the structure-phase and the morphology of the silicon nitride powder used.

Silicon nitride, a highly covalent compound, has two thermodynamically stable phases both having hexagonal structure: the low temperature (<1200 °C) α-phase and the high temperature (>1500 °C) β phase [8]. Between 1200 and 1500 °C both phases coexist. The unit cell dimension of the *c*-axis for α-phase is approximately twice that of the β-phase. The α-phase contains four Si_3N_4 units per unit cell,

* Corresponding author.
E-mail address: kurzina99@mail.ru (I. Kurzina).

1385-8947/$ – see front matter © 2004 Elsevier B.V. All rights reserved.
doi:10.1016/j.cej.2004.12.009

whereas the structural unit of β-phase is Si_6N_8. The β structure is more organized and composed of pickered rings of alternating Si and N atoms having a stacking sequence of ABAB and forming channels with diameters about 1.5 nm along the *c*-direction. The α phase contains the same AB layer and an additional layer CD which is similar to AB except that it is rotated by 180° along the *c*-axis [7,9,10]. It is known that the silicon nitride powder containing higher amounts of α-phase sinters to a material with an higher density compared to the one of β phase [11]. Moreover, the oxidation rate of the silicon nitride depends on the allotropic ratio and the best oxidation resistance at high temperature is achieved for the materials rich in α-phase [12]. Commercial silicon nitride powders are never pure phases and usually contain some amount of a second crystalline variety, up to 15% [7]. The main characteristics such as the specific surface area (S = 5–21 m^2/g), mean particle size, phase composition, thermo-mechanical properties of the commercially available Si_3N_4 powders depend on the production processes [7] and can be influent on the catalytic properties of the systems. It has been shown that Pd and Pt deposited on silicon nitride rich in α-phase have good activity and stability both in total oxidation [13] and in the partial oxidation of methane [14]. Oppositely, the Pd catalyst deposited on silicon nitride, which contained higher amount of β-phase, is inactive and unstable in the total oxidation of methane [15].

Nanosized amorphous silicon nitride powder with much higher specific area (66–100 m^2/g) than α-Si_3N_4 offers a priori considerable advantages and can be used as a support for Pd catalysts. Recently, the properties of platinum catalysts deposited on amorphous silicon nitride were elucidated for the propane dehydrogenation [16]. The obtained catalysts proved to be catalytically active and selective. Moreover, one can expect to produce the silicon nitride powder with the 80–90% crystalline phase content by direct annealing under nitrogen flow at 1420–1500 °C [17] of the amorphous powders keeping a reasonable specific area with changes in the chemical composition, the α/β ratio and the microstructure.

In order to investigate the influence of the phase-structural state of silicon nitride on the catalytic properties of Pd, three kinds of silicon nitride were used as supports in this work: amorphous silicon nitride (SiN-am); amorphous silicon nitride annealed at 1450 °C (SiN-annl) and α-Si_3N_4. The catalytic properties of the resulting systems towards the total oxidation of methane were compared.

2. Experimental

2.1. Supports

Silicon nitride powder materials having different BET specific surface area and phase composition were used as supports of the Pd metal: an amorphous silicon nitride (SiN-am) produced by Johnson Mattey; the same SiN-am treated under nitrogen flow (SiN-annl); and α-Si_3N_4 produced by Goodfellow. The mean support particle size was around 1 μm for α-Si_3N_4 and around 50 nm for SiN-am. After annealing of SiN-am at 1450 °C (SiN-annl) a larger distribution with particles ranging from several tens nm to 1 μm was obtained.

In order to increase the crystalline phase content in an amorphous silicon nitride with still higher specific area than the commercially available α-Si_3N_4, crystallization of the SiN-am was carried out. The properties of amorphous silicon nitride change upon heat treatment in a nitrogen flow in the temperature range 1250–1500 °C for 30–360 min. It was shown that amorphous-to-crystalline phase transition becomes significant above 1380 °C [18,19]. It was suggested the optimum crystallization conditions of the amorphous powder are – temperature, 1450 °C, duration, 120 min [18], these conditions are used in our crystallization experiments.

2.2. Preparation of the catalysts

The catalysts were prepared by impregnation of the supports with adequate amounts of Pd(II) bis acetylacetonate [$Pd(C_5H_7O_2)_2$] dissolved in toluene. Previous works have shown that well-dispersed samples are obtained by such method [13]. After impregnation, evaporation of the solvent and drying at 80 °C, the catalyst precursor was decomposed under argon flow at 500 °C for 2 h, then cooled to RT under Ar. It was then calcined during 2 h at 350 °C under oxygen flow and further reduced under hydrogen flow at 500 °C (in both cases the heating rate was 1 K min^{-1}).

The support particle size did not change during the preparation.

2.3. Supports and catalysts characterization

2.3.1. X-ray diffraction

Phase composition and crystalline state of the silicon nitride supports was controlled by X-ray diffraction using a Bruker D5005 powder diffractometer where the sample is fixed and the X-ray tube (Cu $K_{\alpha 1+\alpha 2}$; λ = 0.154184 nm) and the detector rotates. Each spectrum is acquired in a 2θ range from 3° to 80° using 0.020° steps and acquisition time of 16 s/step.

For the determination of the concentration of different phases, the method of the ratio of intensity with the intensity of reference phase was used [20]. This straight forward method was preferred to more accurate methods than the mean normalized intensity method or the Rietveld full pattern fitting [21] because it is easier to implement. The ratio of concentrations of two phases α and β is proportional to the ratio of diffracted intensities

$$\frac{X_\alpha}{X_\beta} = \frac{I_{\alpha\,\mathrm{norm}}}{I_{\beta\,\mathrm{norm}}}$$

where X_α, X_β are the concentration of α phase and β phase

$$I_{\alpha\,\mathrm{norm}} = \left(\frac{I(h\,k\,l)_\alpha / I(h\,k\,l)_\alpha^{\mathrm{rel}}}{I_\alpha / I_{\mathrm{cor}}} \right),$$

$$I_{\beta\,\mathrm{norm}} = \left(\frac{I(h\,k\,l)_\beta / I(h\,k\,l)_\beta^{\mathrm{rel}}}{I_\beta / I_{\mathrm{cor}}} \right)$$

$I_\alpha/I_{\mathrm{cor}}$ or I_β/I_{cor} ratio of the intensity of the most intense peak of the α or β phase to the intensity of the most intense peak of the reference phase – the corundum (α alumina). This ratio can be found in some PDF files $I_\alpha/I_{\mathrm{cor}} = 0.85$, $I_\beta/I_{\mathrm{cor}} = 1.25$.

The ratio of the amounts of α and β phases is calculated from these averaged intensities using the intensity of the (1 0 1), 20.72Θ; (2 0 1), 31.12Θ and (3 0 1) 43.62Θ peaks of the α phase and (2 0 0), 27.22Θ; (1 0 1), 33.82Θ; (2 1 0), 36.22Θ diffraction peaks of the β phase. The determination of the intensity was performed by integration of diffraction peaks rather than by the simple measurement of their height. The coefficients I/I_{cor} show certain variability compared to the considered PDF files, the average value has been chosen. Note that this approach neglects the possible influence of texture, but can serve as a first guideline.

2.3.2. X-ray photoelectron spectroscopy.

The chemical state of the surface of the silicon nitride supports and of the supported Pd catalysts was checked by XPS. The XPS spectra were obtained on an ESCALAB 200R spectrometer (FISONS Instruments) using the Mg Kα line (1253.6 eV) as an excitation source. The pass energy of the hemispherical electron analyzer was 50 eV, and the angle of the photoelectrons with respect to the plane of the surface was 90°. All data are corrected taking as a reference the N 1s level of Si_3N_4 (397.6 eV). Quantitative analysis of the XPS data was carried out using the software attached to the apparatus, taking into account the atomic sensitivity factors, the transmission of the analyzer and the photoelectrons mean paths in the material.

2.3.3. Transmission electron microscopy

The morphology of the silicon nitride supports and Pd catalysts was studied by the transmission electron microscopy (TEM). The microscope is a JEOL JEM 2010, operating at 200 kV, equipped with a LaB_6 tip, a high resolution polepiece and a Pentafet-LinK ISIS EDS-X spectrometer (Oxford Instruments). The samples were dispersed in ethanol. A drop of this suspension was disposed on a holey-carbon thin film supported on a microscopy copper grid (3.05 mm, 200 mesh). The palladium particle size was determined from the TEM images. The average particle size was calculated.

2.3.4. BET

Specific BET surface areas were determined by argon adsorption using an home made automatic adsorption apparatus.

2.3.5. Chemical analysis

Induced coupled plasma (ICP) chemical analysis has been used to determine the metal contents. The palladium from the samples was dissolved in a mixture $H_2SO_4/HNO_3/HF$ at 250 °C and HF + (2/3)HCl/(1/3)HNO_3 at 150–200 °C. The acidic treatment did not dissolve completely the silicon nitride support and a white-gray residue was observed. The solutions were filtered before analysis by optical ICP in a SPECTRO monochromatic spectrophotometer (Pd wavelength 340.6 nm).

2.3.6. Catalytic measurements

The total oxidation of methane was carried out between 25 and 650 °C in a flow tubular quartz reactor (diameter = 2 cm) with a stationary layer of catalyst. The temperature of the catalysts was measured using a thermocouple with its end in the catalytic bed. The catalytic bed was nearby 2 mm and located in the middle of the furnace (30 cm length). A 0.2 g mass loading of catalyst was used for each experiment. The flux of reactants (methane, oxygen and nitrogen in ratio 2.5/19.5/78) was maintained at 100 ml/min (a time of contact was 0.9 s^{-1}). The products were analyzed by mass-spectrometry. CO_2 and H_2O were the only products. Methane conversion versus temperature was measured for two states of the samples noted respectively:

State 1. As prepared catalysts, the rate of the temperature increase was fixed at 3°/min.
State 2. The samples heated 3 h at 650 °C in the presence of the reagents mixture; the rate of increasing temperature was 1°/min.

3. Results and discussion

3.1. Supports

3.1.1. Amorphous silicon nitride

Physico-chemical properties of the silicon nitride powders as studied by XRD, XPS and TEM are presented in

Table 1
Characteristics of silicon nitride powder selected for investigation

Samples	BET Spes. area ($m^2\,g^{-1}$)	XRD data		XPS data		
		Amorphous fraction	α/β phases ratio	SiO_x (%) from Si 2p	[Si]/[N]	[N] + [O]/[Si]
SiN-am	66	Majority	2.3	22	1.16	1.65
SiN-annl	28	Small amount	6.6	6	1.14	1.33
α-Si_3N_4	7	Traces	5.8	13	1.28	1.36

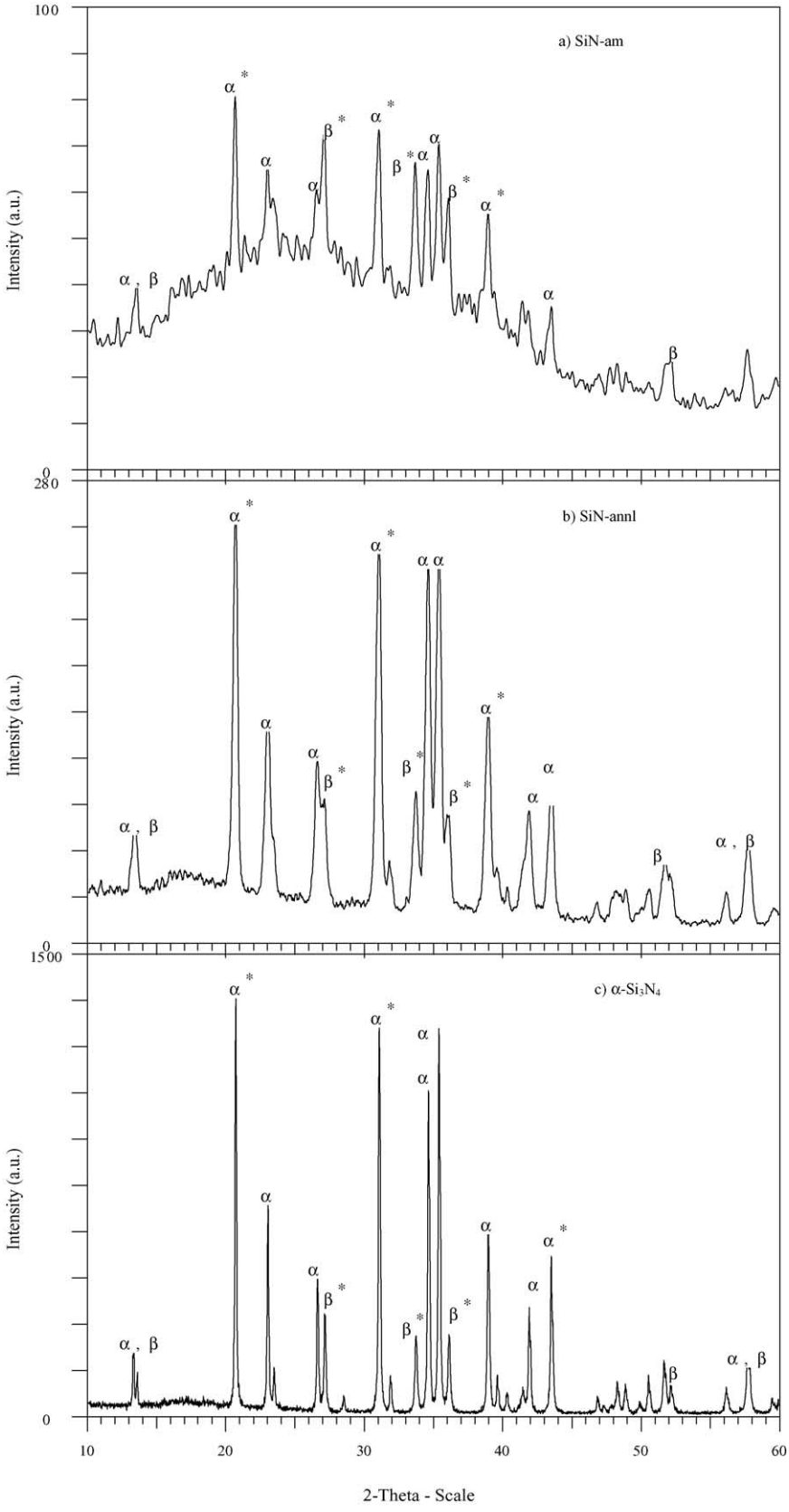

Fig. 1. X-ray diffraction patterns of the silicon nitride supports.

Table 1. The SiN-am support has a greater specific surface area 66 m^2/g as compared to that of α-Si_3N_4 (7 m^2/g) (Table 1). Fig. 1a shows the X-ray diffractogram of the amorphous silicon nitride powder. The powder was mainly amorphous with a small amount of crystalline phase. The X-ray phase analysis shows that the crystalline fraction consists of α-phase, besides this phase β-phase also exists. The α/β ratio = 2.3 (Table 1) demonstrating the dominance of α phase in the crystalline fraction.

TEM investigation of amorphous silicon nitride sample was undertaken. The TEM images showed that the amorphous silicon nitride sample consisted of rather uniform, quasi-spherical particles of amorphous fraction with the mean particle size about 20 nm. However, these particles tend to agglomerate to some extent. Some silicon nitride crystals also exist among the amorphous particles.

The chemical states of the surface were detected by XPS. The binding energy positions of the Si 2p and N 1s peaks are 101.9 and 397.6 eV, as expected for Si and N atoms in Si_3N_4. The surface composition of the amorphous silicon nitride is presented in Fig. 2a. A small amount of carbon is present on the surface; a very low [C]/[Si] ratio of 0.09 was determined by XPS. The ratio of [Si]/[N] is higher than the stoichiometry of Si_3N_4 (0.75) (Table 1), which mean that amorphous material does not have ideal composition. The ideal structure of amorphous silicon nitride by theoretical calculations was described in [22]. Model of amorphous phase contains no "wrong" bonds (only Si–N, Si–Si bond) and perfect coordination. The structure contains pores of about 650 pm surrounded by a framework of α-Si_3N_4 [23]. In real situation, amorphous silicon nitride contains some amount of oxygen or other impurities like H which can be dissolved in the struc-

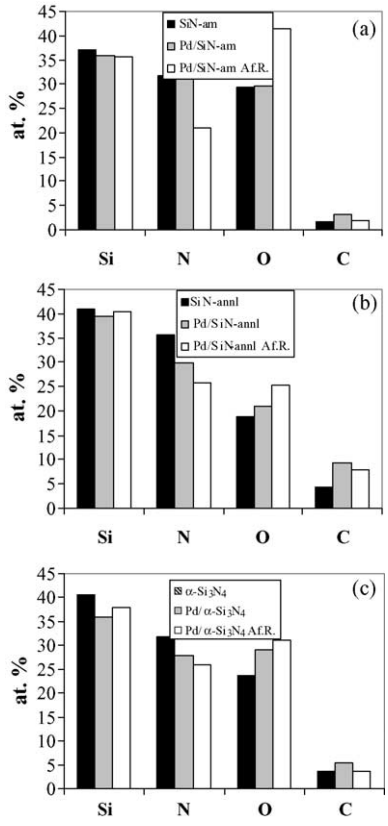

Fig. 2. The elemental composition of the surface of the Pd/SiN-am (a), Pd/SiN-annl (b) and Pd/a-Si_3N_4 (c).

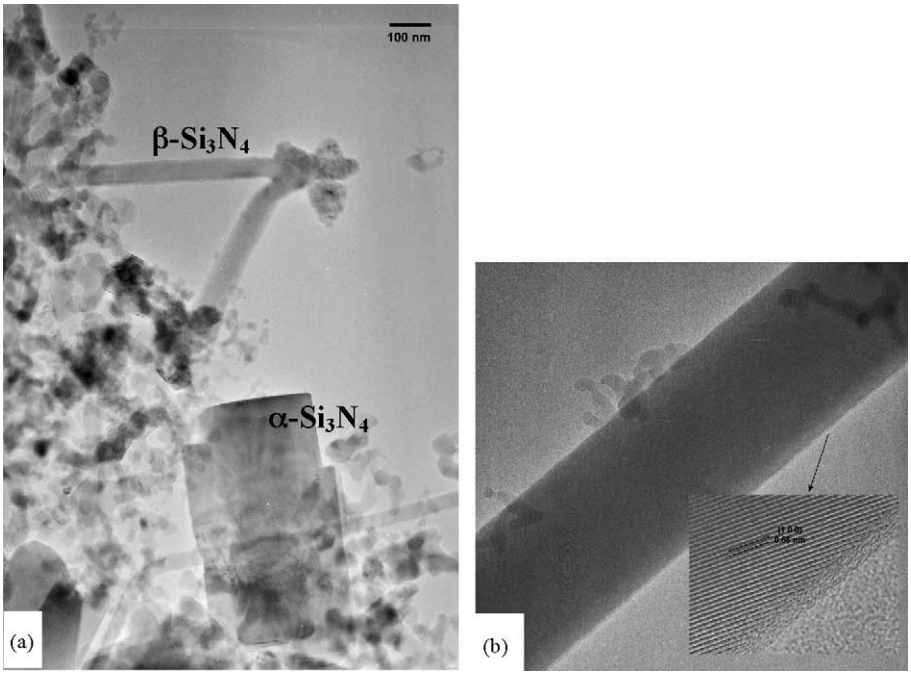

Fig. 3. Morphology of the amorphous silicon nitride annealed (SiN-annl) (a), structure of the β-phase whiskers (b).

ture of silicon nitride or substitute the Si or N atoms in the amorphous framework. The stoichiometry of amorphous silicon nitride can be expressed as $Si_{1-x}N_x{:}H_y$ [24] and can also have the composition $Si–N_{4(1-x)/3}\ O_{2x}$. Nitrogen and oxygen atoms are bonded to 3 and 2 silicon atoms, respectively [25]. The XPS peak of Si 2p can be decomposed into two contributions of the silicon in Si_3N_4 and SiO_2 compounds. The signal corresponding to the SiO_2 represents about 22% of the total Si signal (Table 1). The ratio [O] + [N]/[Si] = 1.65 is very close to the stoichiometry $Si–N_{4(1-x)/3}O_{2x}$.

3.1.2. Annealed amorphous silicon nitride

XRD spectrum of silicon nitride treated under nitrogen flow is given in Fig. 1b. The amorphous fraction decreased and thus, the powder became more crystalline. In the respective XRD pattern one can see that the amorphous fraction did not disappear entirely. The peaks assigned to α and β phases are stronger than in amorphous powder. The α/β ratio increased up to 6.6 (Table 1).

The specific surface area decreased from 66 to 28 m^2/g after annealing under nitrogen flow. Crystallization is associated with grain coarsening as it is shown by changes of the specific area and also by results of TEM (Fig. 3). The evolution of the microstructure and crystalline phase of the silicon nitride powder was monitored. Contrary to Ref. [26] there is also formation of whiskers in nitrogen atmosphere with structure more close to β phase. The TEM images of the material indicated that the whiskers structure is surrounded by an amorphous sheath of about 1 nm thickness.

The annealing atmosphere and other factors like the crystalline phase contents and the heat-treatment of the powder have an effect on the formation of whiskers having the β phase structure [18] It also shown that treatment in nitrogen can promote whisker (β-Si_3N_4) formation [18,27,28]. Particularly, the phase ratio and crystallite size of α and β-phase in the starting powder have been found to be the key factors in the microstructure development [7]. During the sintering the Si_2N_2O phase can be produced and that can transform with α-phase to β-Si_3N_4. Moreover, both α and β phase can be crystallized from amorphous phases.

From XPS data one can see (Fig. 2), that the nitrogen content slightly increases compare to amorphous silicon nitride due to the oxygen removal and nitration of the present silicon. As shown in Table 1, the support pretreatment leads to a significant decrease of the oxygen content 6 at.% (by deconvolution of Si 2p peak). The calculation of [N] + [O]/[Si] = 1.33 from XPS data shows that the thermal treatment in nitrogen atmosphere results in the products with the stoichiometric composition very close to Si_3N_4 ([Si]/[N] = 1.33). The oxygen does not belong to structure of silicon nitride, it can be present on the surface like SiO_2 with thickness 0.3 nm (from comparing of intensity of Si 2p peaks).

3.1.3. α-Si_3N_4

The XRD spectrum of α-silicon nitride support is presented in Fig. 1c. No broad peaks (e.g. like those visible on the XRD pattern of the SiN-am) characteristics of an amorphous state were observed on the background spectrum. Conversely to other samples, α-silicon nitride shows narrow and intense diffraction peaks which are characteristic features of a very well crystallized material. The main lines correspond to the α-phase, some amount of β-phase was also detected, with concentration not exceeding of 15 wt.%. The ratio of α/β phases is about 5.8 (Table 1) and less than in a crystalline part of SiN-annl powder. In addition, a certain amount of crystalline Si was found in this powder with concentration of 0.5 wt.%.

TEM investigation of silicon nitride sample was undertaken. The TEM images showed that the silicon nitride sample consisted of uniform, spherical particles with the mean particle size about 1 μm. The presence of oxygen on the surface was detected by XPS. By deconvolution of Si 2p signal was shown that 13% correspond to SiO_2. It was calculated from the XPS data that the stoichiometry ([O] + [N])/[Si] in α-phase specimen is 1.36 and close to [N]/[Si] in Si_3N_4.

There is a lot of discussion in the literature about the structure of α-silicon nitride. Until recently, the composition and the structure of α-Si_3N_4 has been the subject of controversy. Wild et al. proposed in agreement with their structural determination and supported by oxygen analyses, that this phase was actually a silicon nitride oxynitride phase, where oxygen substitute some nitrogen atoms and silicon sites are vacant [29]. Jack suggested that the α-Si_3N_4 structure might be stabilized by the occurrence of Si^{3+} interstitials, the valence being compensated by oxygen atoms [30]. Hence, the α-Si_3N_4 phase can be represented on the thermochemical diagrams as an intermediate material of composition $SiN_{1.32}O_{0.03}$ (at 2% of oxygen). Some authors recently proved that although oxygen atoms might substitute nitrogen in α-Si_3N_4, there is no structural requirement for its presence. For instance, oxygen concentration as low as 0.05 wt.% was measured in an α-Si_3N_4 single crystal.

The presence of oxygen in the surface of α-silicon nitride support can be attributed to the superficial SiO_x. Comparison of the intensity of Si 2p peaks which correspond to SiO_2 and Si_3N_4 phases, suggests that thickness of the possibly superficial layer of silicon oxide does not exceed 0.8–1 nm. Moreover, it is possible that the oxygen detected by XPS belongs to the presence of $Si–N_3O$ tetrahedrons embedded on the surface of the structure of the α-Si_3N_4 [25].

3.2. Pd catalysts deposited on silicon nitride

For the Pd catalysts deposited on silicon nitride supports the Pd content was chosen to be near 0.50 wt.%. This value is sufficient for physical characterization but not too large, thus allowing us to expect a good dispersion of Pd. In order to obtain such an amount of metal we had to be aware that a constant loss of about 0.15 wt.% occurs during preparation and so we had to make the preparation with an initial amount of 0.65 wt.%. Indeed, following the preparation, the values of the amount of deposited Pd measured by chemical analysis

Table 2
Main characteristics of the Pd/silicon nitride catalysts

Samples	Pd content (wt.%) ± 0.008		TEM average particle size (nm)		BE Pd $3d_{5/2}$ (eV)		Pd 3d (%)/Si 2p (%)		SiO_x (%) from Si 2p		Half-conversion temperatures	
	B.R.	Af.R.	B.R.	Af.R.	B.R.	Af.R.	B.R.	Af.R.	B.R.	Af.R.	State 1	State 2
Pd/SiN-am	0.44	0.43	2.9	3.2	335.3	337.0	0.0046	0.0048	22	40	430	530
Pd/SiN-annl	0.42	0.42	3.2	3.6	335.9	337.3	0.0106	0.0117	15	18	370	470
Pd/α-Si_3N_4	0.49	0.49	4.3	5.8	335.9	337.3	0.044	0.038	22	24	360	360

BE: binding energy; B.R.: catalyst before reaction; Af.R.: catalyst after reaction.

were in the range 0.42–0.49 wt.% thus being close to the expected ones (Table 2) for all the samples.

The XRD patterns of Pd/silicon nitride catalysts are very similar to those of the supports. It means that no significant modification of the support occurs during the catalyst preparation and reaction. The lines of the Pd in the XRD spectrums have very low intensity due to less amount of metal. The TEM pictures of the three Pd/silicon nitride catalysts were undertaken. The Pd particles have nanosize (2.9–4.3 nm) and well distributed on the surface. The slight increase of the average Pd particles size for as prepared catalysts simultaneous with the decrease of the specific surface areas of the supports was observed (Table 2).

The curves showing CH_4 conversion of the Pd/SiN-am, Pd/SiN-annl and Pd/α-Si_3N_4 as a function of increasing temperature at states 1 and 2 are given in Fig. 4a and b, respectively. Under reaction treatment (states 1 and 2) no relevant modification of the Pd/α-Si_3N_4 activity was recorded. In the state 1 Pd/SiN-annl sample exhibits a catalytic behavior quite comparable to the Pd/α-Si_3N_4, a half-conversion temperature is quite the same, being near 360–370 °C (Table 2). However, after aging at 650 °C under the gas mixture (state 2), a significant decrease of activity is observed (Fig. 4b). The light-off temperature (at half-conversion) increases from 370 to 470 °C (Table 2). The Pd/SiN-am catalyst shows a lower activity by comparison with the other samples in the state 1 and moreover the activity decreases under the reaction conditions, the conversion of methane in state 2 not rich up to 100%. The increase of the temperature of the half-conversion from 430° (state 1) to 530° (state 2) was found (Table 2). In principle, this catalyst should be rather active since catalysts supported on materials with high specific area show better activity for oxidation of hydrocarbons.

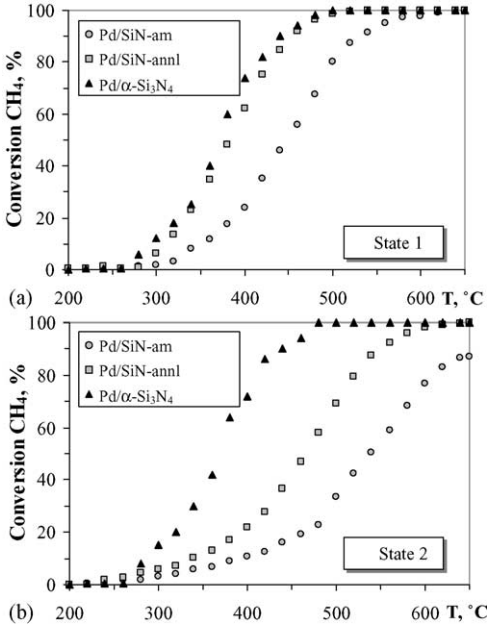

Fig. 4. Methane conversion over Pd/SiN-am; Pd/SiN-annl; Pd/α-Si_3N_4 catalysts according to their "states" of reaction: state 1 (a); state 2 (b).

The catalytic difference in reaction in state 1 can be explained with respect to the properties of the Pd particles. The surface structures of small metallic particles and electronic state are determined by their shapes which depend on the nature of the support. The Pd $3d_{5/2}$ binding energy measured on the three catalysts as prepared and after attaining state 2 are reported in Table 2. The binding energy of the fresh Pd/SiN-am is 335.3 eV and comparable to that of pure palladium (335.4 ± 0.1 eV) obtained with the same XPS device [31]. The binding energy of Pd $3d_{5/2}$ for the as-prepared Pd/SiN-annl and Pd/α-Si_3N_4 are shifted towards higher energy (335.9 eV). This effect cannot be explained by oxidation of Pd in ambient atmosphere before XPS, the line shape of both the Pd 3d XPS peaks and the corresponding Auger spectrum is quite comparable to that obtained for a reduced Pd° state as measured for a clean and massive palladium sample and not to an oxidized Pd^{2+} state. It cannot be explained also by a size effect [13,32] since TEM indicates a mean diameter of Pd particles exceeding 2.5–3 nm.

The value of Pd $3d_{5/2}$ (336.1 eV) instead of 335.3–335.4 eV for Pd metal was also found for Pd (0.75%)/α-Si_3N_4 catalyst [13] and it is quite higher than for Pd deposited on SiO_2, SiC, Al_2O_3. It has to be added that the binding energy for Pd/α-Al_2O_3 corresponds to pure Pd metal (335.2 eV) [13]. One can thus propose that these higher values are induced by some modification of the electronic properties of the Pd particle due to support interaction. Some special interaction between palladium and α-phase of silicon nitride leads to modifications of electronic and/or structural properties of the metal. Moreover, it can depend on the crystalline state of silicon nitride.

The decrease of activity for Pd/SiN-am and Pd/SiN-annl in state 2 cannot be explained by the oxidation of Pd metal to PdO since the latter is expected to be more active. Indeed, the increase of the Pd $3d_{5/2}$ binding energy (337–337.3 eV)

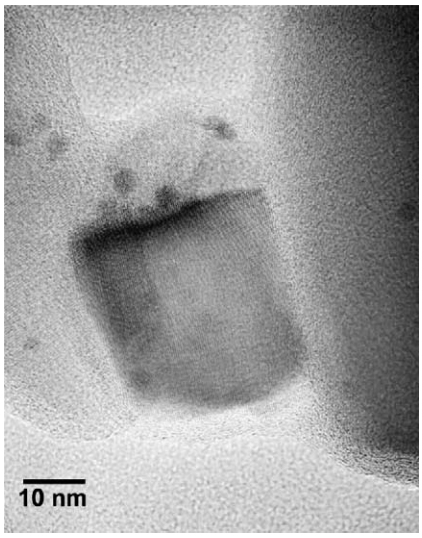

Fig. 5. TEM pictures of Pd/SiN-annl after reaction.

was found for all catalysts after reaction, including Pd/α-Si_3N_4 catalyst (Table 2), suggesting that in all cases the phase present during reaction is the oxide one, as expected. These values of Pd $3d_{5/2}$ binding energy are very close to those for PdO (336.8 ± 0.1 eV) [31]. The deactivation of the Pd/SiN-am and Pd/SiN-annl catalysts also cannot be explained by sintering of metallic particles. The resistance of the palladium metallic particles to sintering under reaction can be confirmed by the lower increase of the [Pd]/[Si] ratio after reaction (Table 2).

The decreasing of activity for Pd/SiN-am and Pd/SiN-annl in state 2 can be explained by the presence of amorphous fraction in the supports and its oxidation resistance. Under reaction conditions at high temperature, silicon nitride may undergo peculiar processes: the oxidation of the support amorphous part, moving of the amorphous matter and following coverage of the metallic particles. These processes can take place during reaction over Pd/SiN-am catalyst. The Si 2p and O 1s XPS peaks changed in shape and intensity after reaction for Pd/SiN-am, indicating that oxidation of the silicon nitride support has occurred. The oxygen content increased by a factor of two after reaction (Fig. 2). For Pd/SiN-annl catalyst the increasing of the oxygen content was not obtained (Fig. 2), it means that no oxidation of the support has occurred. The presence of amorphous fraction near the crystals leads to the coverage of the metallic particles under reaction, which is confirmed by TEM investigations. It is visible in Fig. 5 that after reaction some regions with Pd particles deposited on the crystalline fraction of SiN-annl are completely covered by the amorphous fraction.

4. Conclusion

On the base of the results obtained in this work, the following conclusions can be made:

- XRD analysis was used in combination with TEM and XPS analysis to determine the composition and the structure of amorphous silicon nitride, the same sample after annealing under nitrogen flow and α-Si_3N_4. The amorphous silicon nitride containing small amounts of crystalline fractions (with α/β ratio of 2.3) has the higher specific area and contains the greater amount of oxygen. The effect of crystallization on the phase content and morphology of the amorphous silicon nitride was studied. After treatment at 1450° under nitrogen flow, the crystalline fraction containing both α and β phases became very high and the increasing of the α/β ratio 6.6 after annealing was observed. The formation of whiskers with structure close to β-phase was established. The α-Si_3N_4 sample was found to be a very well crystallinzed material containing mainly α-Si_3N_4 with a ratio α/β ratio of 5.8 and traces of amorphous fraction.
- The preparation of Pd (0.5 wt.%) catalysts by impregnation $Pd(AcAc)_2$ on silicon nitride supports (SiN-am, SiN-annl, α-Si_3N_4) leads to the formation of nanosized metal particles. Pd catalysts show different catalytic activity for the total oxidation of methane. It increases with the α-Si_3N_4 content and crystallization state of the support. This behavior can be due to the modification of the electronic states or the structure of the Pd metallic particles depending on the nature of the silicon nitride. The XPS Pd $3d_{5/2}$ – binding energy depends on the support: it is higher for Pd/SiN-annl and Pd/α-Si_3N_4. It can be explained by a specific interaction between Pd metal and α-Si_3N_4 phase. The decrease of the catalytic activity is observed for Pd/SiN-am and Pd/SiN-annl. It was proposed that the decreasing of the activity can be explained by the presence of the amorphous fraction in the support which can easier be oxidized and move at high temperatures [33]. Pd/α-Si_3N_4 was found to be active and stable under reaction condition.

Acknowledgements

The authors gratefully thank Marie-Thérèse Gimenez for the preparation of the catalysts; Michèle Brun is greatly acknowledged for the XPS experiments as well as Alain Bonnetot for the high temperature treatment under nitrogen flow of the amorphous silicon nitride sample.

References

[1] V.I. Bukhtiyarov, M.G. Slin'ko, Russ. Chem. Rev. 70 (2) (2001) 147.
[2] A. Vannice, Y.L. Chao, R.M. Friedman, Appl. Catal. 20 (1986) 91.
[3] Ch. Méthivier, B. Béguin, M. Brun, J. Massardier, J.C. Bertolini, J. Catal. 173 (1998) 374.
[4] P.W. Ladnor, R. De Ruiter, J. Chem. Soc., Chem. Commun. (1989) 520.
[5] P. Grange, P. Bastians, R. Conanec, R. Marchand, Y. Laurent, Appl. Catal. A 114 (1994) L191.

[6] N. Fripiat, P. Grange, Chem. Commun. (1996) 1409.
[7] W. Dressler, R. Riedel, Int. J. Reflect. Met. Hard Mater. 15 (1997) 13.
[8] D.R. Messier, W.J. Croft, Silicon nitride, in: W.R. Wilcox (Ed.), Preparation and Properties of Solid State Materials, vol. 7, Marcel Dekker, New York, 1982, p. 173.
[9] S. Hampshire, H.K. Park, D.P. Thompson, K.H. Jack, Nature 274 (1978) 880.
[10] R. Grun, Acta Cryst. 35 (1979) 800.
[11] S. Kumar, K. Khosla, B.T. Rao, T.R. Rama, Mohan, J. Mater. Sci. 22 (1987) 3041.
[12] B.P. Butt, D. Albert, T.N. Taylor, J. Am. Ceram. Soc. 79 (11) (1996) 2809.
[13] C. Méthivier, J. Massardier, J.C. Bertolini, Appl. Catal. A: General 182 (1999) 337.
[14] F. Monnet, Y. Schuurman, F. Cadete Santos Aires, J.C. Bertolini, C. Mirodatos, Catal. Today 64 (2001) 51.
[15] F.J. Cadete Santos Aires, G. Garcia Cervantes, P. Delichère, J.-C. Bertolini, in: IBP, SBC (Eds.), Novas Fronteiras em Catálise, Anais do 12 Congresso Brasileiro de Catálise, Brasilio, 2003, p. 836.
[16] D. Hullmann, G. Wendt, U. Singliar, G. Ziegenbalg, Appl. Catal. A: General 225 (2002) 261.
[17] J. Szépvölgyi, I. Tóth, T. Székely, Proceedings of the ISPC-9, vol. 11, Pugnochiuso, Italy, 1989, p. 727.
[18] F. Allair, R. Langlois, J. Mater. Sci. 27 (1992) 1265.
[19] R. Brink, H. Lange, Key Eng. Mater. 89–91 (1994) 73.
[20] R. Jenkins, R.L. Snyder, Introduction to X-ray Powder Diffractometry, Wiley, New York, 1996, Chapter 13, p. 355.
[21] H. Toraya, J. Appl. Cryst. 32 (1999) 704.
[22] P. Kroll, J. Non-Cryst. Solids 293–295 (2001) 238.
[23] T. Searle (Ed.), Properties of Amorphous Silicon and its Allows, INSPEC, London, 1998.
[24] R.C. Weast (Ed.), Handbook of Chemistry and Physics, 67th ed., CRC, New York, 1986.
[25] G. Chollon, R. Hany, U. Vogt, K. Berroth, J. Eur. Ceram. Soc. 18 (1998) 535.
[26] J. Szépvölgui, I. Mohai, Ceram. Int. 25 (1999) 711.
[27] J. Gubicza, J. Szépvölgui, I. Mohai, L. Zsoldos, T. Ungár, J. Mater. Sci. 35 (2000) 3711.
[28] X.C. Wu, W.H. Song, B. Zhao, W.D. Huang, M.H. Pu, Y.P. Sun, J.J. Du, Solid State Commun. 115 (2000) 683.
[29] S. Wild, P. Grievson, K.H. Jack, The British Ceramic Research Association, Stoke on Trent, UK, 1992, p. 385.
[30] K.N. Jack, In progress in nitrogen ceramics, in: F.L. Riley (Ed.), Martinus Nijhoff, Hague, The Netherlands, 1983, p. 45.
[31] M. Brun, A. Berthet, J.C. Bertolini, J. Elect. Spectros. Relat. Phenom. 104 (1999) 55.
[32] S. Kohiki, Surf. Sci. 25 (1986) 81.
[33] K. Kijima, S. Shirasaki, J. Chem. Phys. 65 (1976) 2668.